Discrete Differentiators Based on Sliding Modes ⋆

Jean-Pierre Barbot [a], Arie Levant [b,⋆⋆], Miki Livne [c], Davin Lunz [d]

[a] *Quartz EA 7393, ENSEA, Cergy-Pontoise, France*

[b] *School of Mathematical Sciences, Tel-Aviv University, Israel*

[c] *Israel Aerospace Industries, Israel*

[d] *Mathematical Institute, University of Oxford, UK*

Abstract

Sliding-mode-based differentiation of the input $f(t)$ yields exact estimations of the derivatives $\dot{f},...,f^{(n)}$, provided an upper bound $L(t)$ of $|f^{(n+1)}(t)|$ is available in real-time. In practice it involves discrete sampling and numerical integration of the internal variables between the measurements. Accuracy asymptotics of different discretization schemes are calculated for discrete noisy sampling, whereas sampling and integration steps are independently variable or constant. Proposed discrete differentiators restore the optimal accuracy asymptotics of their continuous-time counterparts. Event-triggered sampling is considered. Extensive numeric experiments are presented and analyzed.

Key words: Differentiators, Sliding mode, Sampled signals, Digital filters, Accuracy.

1 Introduction

Differentiation of noisy signals is usually performed by the algebraic, functional-analysis [31] and control/observation methods. The observation-approach is to approximate the input by a signal with known derivatives to be considered as derivatives' estimations. Such tracking is often based on high-gain [3], homogeneous [34] and sliding-mode (SM) control [44,12,41,45]. High-order sliding modes (HOSMs) [5,7,11,13,15,19,29,35,36,33,39,42] require finite-time (FT) exact robust differentiators and use homogeneity theory for their development [2,9,19,20,32,37,40].

Homogeneous SM-based differentiators [19,22] provide for the FT exact estimation of the derivatives $f^{(i)}, i \le n$, of the input $f(t)$, provided an upper bound L, $|f^{(n+1)}| \le L$, is available. They also provide for the optimal error asymptotics with respect to the noise magnitude [27] (see Section 3.1). Differentiators [25,28] also reject *unbounded* noises of small average value. Variable $L(t)$ is considered in [10,22,24].

A practical SM-based differentiator is a computer-based system with a noisy discretely-sampled continuous-time input, and numerical integration of the discontinuous dynamics over each sampling interval [30,38]. Its error dynamics are in fact hybrid [43,30].

The widely used Matlab solvers are based on the Runge-Kutta methods and are not applicable to SM-based dynamics due to accuracy deterioration and slow calculation. Thus the Euler method becomes the main integration method in application and simulation of such systems.

One naturally expects the vanishing Euler integration step to restore the optimal error asymptotics [19,20] obtained in the continuous-time case. That expectation is mathematically true, but we prove here that *it is practically impossible to choose a sufficiently small integration step if the differentiation order n exceeds* 1.

Novelty. This paper is the first regular publication analyzing the influence of intermediate integration steps in the discrete SM-based differentiation. We prove and demonstrate some of the results briefly announced at the conference [6] and, without proofs, in the survey book chapter [26]. In contrast to [6,26] we also introduce new homogeneous-discretization methods, consider variable parameter $L(t)$ for differentiators [19] and extend the results to the non-homogeneous hybrid differentiators recently introduced in [24].

The proposed new methods of homogeneous discretization significantly extend results of [30] and restore the optimal continuous-time accuracy asymptotics [19,22,27] for considered differentiator types. In that particular case the intermediate integration steps are shown to neither destroy nor improve the accuracy asymptotics.

A special implementation case corresponds to the input produced by an event-triggered sensor, since the sampling-time intervals become unbounded. Differentiation of such signals by SM-based technique is a long-standing problem. As a solution we propose a simple virtual-measurements' strategy removing the possible differentiation instability and even providing for the optimal accuracy asymptotics.

The paper structure. The weighted homogeneity theory and SM-based differentiators are briefly introduced in Sections 2, 3. Theoretical results are presented in Sections 4, 5. Extensive numeric experiments are analyzed in Section 6. All proofs are concentrated in appendices.

Notation. Denote $\lfloor A \rceil^B = |A|^B \operatorname{sign} A$ if $B > 0$ or $A \neq 0$; $\lfloor A \rceil^0 = \operatorname{sign} A$. Let $f(\Omega) = \{f(\omega) \mid \omega \in \Omega\}$ for any set Ω and function f. For any sets Ω, Θ and the binary operation $\diamond$ define $\Omega \diamond \Theta = \{\omega \diamond \theta \mid \omega \in \Omega, \theta \in \Theta\}$, also $\omega \diamond \Theta = \{\omega\} \diamond \Theta$.

$||\cdot||$ is the Euclidean norm, $B_\varepsilon = \{x| \, ||x|| \le \varepsilon\}$. The upper semi-continuity of a compact-set function $F(x)$, $F: \mathbb{R}^k \to 2^{\mathbb{R}^k}$, means that the maximal distance from the points of $F(x)$ to the set $F(y)$ tends to zero, as $x \to y$.

A statement is said to hold *for sufficiently small (large)* $v_1,...,v_k > 0$, if there exist such $w_1,...,w_k > 0$ that it holds for any $v_1 \le w_1,...,v_k \le w_k$ (respectively $v_1 \ge w_1,...,v_k \ge w_k$).

⋆ Accepted October 03, 2019
https://doi.org/10.1016/j.automatica.2019.108633

⋆⋆Corresponding author: Arie Levant. Email: levant@tauex.tau.ac.il.

2 Weighted homogeneity of differential inclusions

Let $T_x\mathbb{R}^{n_x}$ denote the tangent space to $\mathbb{R}^{n_x}$ at the point x. Recall that a solution of a differential inclusion (DI)

$$\dot{x} \in F(x),\ x \in \mathbb{R}^{n_x},\ F(x) \subset T_x\mathbb{R}^{n_x}, \tag{1}$$

is defined as any locally absolutely continuous function $x(t)$, satisfying the DI for almost all t. DI (1) is called *Filippov DI*, if $F(x)$ is non-empty, compact and convex for any x, and F is an upper-semicontinuous set function.

Filippov DIs feature existence and extendability of solutions, but not the solution uniqueness [14].

Introduce the weights $m_1, m_2, \dots, m_{n_x} > 0$ of the coordinates $x_1, x_2, \dots, x_{n_x}$ in $\mathbb{R}^{n_x}$. Define the dilation $d_\kappa(x) = (\kappa^{m_1}x_1, \kappa^{m_2}x_2, ..., \kappa^{m_{n_x}}x_{n_x})$ for $\kappa \geq 0$.

Recall [4] that a function $f: \mathbb{R}^{n_x} \to \mathbb{R}^m$ is said to have the homogeneity degree (weight) $q \in \mathbb{R}$, $\deg f = q$, if the identity $f(x) = \kappa^{-q} f(d_\kappa x)$ holds for any x and $\kappa > 0$. We do not distinguish between the weight of the coordinate x_i and the homogeneity degree of the coordinate function $c_{x_i}(x) = x_i$: $\deg c_{x_i} = \deg x_i = m_i$.

A vector-set field $F(x) \subset T_x\mathbb{R}^{n_x}$ (DI (1)) is called *homogeneous of the degree* $q \in \mathbb{R}$, $\deg F = q$, if the identity $F(x) = \kappa^{-q} d_\kappa^{-1} F(d_\kappa x)$ holds for any x and $\kappa > 0$ [20].

Hence, the homogeneity of the vector-set field $F(x) \subset T_x\mathbb{R}^{n_x}$ implies the invariance of DI (1) with respect to the combined time-coordinate transformation $(t,x) \mapsto (\kappa^{-q}t, d_\kappa x)$, $\kappa > 0$, where $-q$ can be considered as the weight of t, $\deg t = -q$.

The standard definition [4] of homogeneous differential equations is a particular case here. Note the difference between the homogeneity degree of a vector function taking values in $\mathbb{R}^{n_x}$ and of a vector field which takes the values in the tangent space $T\mathbb{R}^{n_x}$.

The non-zero homogeneity degree q of a vector-set field can always be scaled to ± 1 by an appropriate proportional change of the coordinate weights $m_1, ..., m_{n_x}$.

The *contractivity* [20] of the homogeneous Filippov DI (1) is equivalent to the existence of $T > 0$, $R > r > 0$, such that for all solutions $||x(0)|| \leq R$ implies $||x(T)|| \leq r$.

A Filippov DI $\dot{x} \in \tilde{F}(x)$ is called a *small homogeneous perturbation* of (1) if $\deg F = \deg \tilde{F}$, and $F(x) \subset \tilde{F}(x) + B_\varepsilon$, $\tilde{F}(x) \subset F(x) + B_\varepsilon$ hold for some small $\varepsilon \geq 0$ and any $x \in B_1$.

Theorem 1 ([23,21]) *Let the Filippov DI* (1) *be homogeneous,* $\deg F = q$. *Then its asymptotic stability and contractivity features are equivalent and robust to small homogeneous perturbations. If* $q < 0$ *the asymptotic stability implies the FT stability. Moreover, the FT stability of* (1) *implies that* $q < 0$.

3 SM-based differentiation

Assumption 1 ***a:*** *The input* $f(t) = f_0(t) + \eta(t)$ *consists of a bounded Lebesgue-measurable noise* $\eta(t)$ *and an unknown basic signal* $f_0(t)$ *with the locally Lipschitzian nth derivative satisfying* $|f_0^{(n+1)}| \leq L_0(t)$ *for almost all t and a locally absolutely continuous function* $L_0(t) > 0$. ***b:*** *The ratio* η/L_0 *is bounded,* $|\eta|/L_0(t) \leq \varepsilon$. *The number* $\varepsilon \geq 0$ *is unknown.*

Assumption 2 *In its turn* $L_0(t)$ *is provided by the additional input* $L(t)$, $L(t) > 0$, $L(t) = L_0(t) + \eta_L(t)$, *where* $\eta_L(t)$ *is a Lebesgue measurable noise,* $|\eta_L(t)|/L_0(t) \leq \varepsilon_L$, *and* $L_0(t) > 0$, $|\dot{L}_0(t)|/L_0(t) \leq M$. *The number* $M \geq 0$ *is known,* $\varepsilon_L \in [0,1)$ *is unknown.*

The problem is to evaluate the derivatives $f_0^{(i)}(t)$, $i = 0, 1, ..., n$, in real time.

For example, in the case of the gain-scheduled control (e.g. in flight control), when the system with the output $f(t)$ is locally approximated by linear models, $L(t), M$ are roughly determined by the model matrices and the control. The corresponding function $L(t)$ is discontinuous.

In the case of constant L we assume that $\varepsilon_L = 0$, $L = L_0$.

3.1 Homogeneous SM-based differentiators

In this subsection we assume that $L = L_0$ *is constant,* $M = 0$. The following is the recursive form of the differentiator [19]. Its outputs z_j estimate the derivatives $f_0^{(j)}$, $j = 0, \dots, n$, in FT for constant $L = L_0$, $M = 0$, $\varepsilon_L = 0$:

$$\begin{aligned}
\dot{z}_0 &= -\lambda_n L^{\frac{1}{n+1}} \lfloor z_0 - f(t) \rceil^{\frac{n}{n+1}} + z_1, \\
\dot{z}_1 &= -\lambda_{n-1} L^{\frac{1}{n}} \lfloor z_1 - \dot{z}_0 \rceil^{\frac{n-1}{n}} + z_2, \\
&\dots \\
\dot{z}_{n-1} &= -\lambda_1 L^{\frac{1}{2}} \lfloor z_{n-1} - \dot{z}_{n-2} \rceil^{\frac{1}{2}} + z_n, \\
\dot{z}_n &= -\lambda_0 L \operatorname{sign}(z_n - \dot{z}_{n-1}).
\end{aligned} \tag{2}$$

An infinite sequence of parameters $\lambda_i > 0$ can be built starting from any $\lambda_0 > 1$, which is valid for *all* natural n [19]. In particular, one can choose $(\lambda_0, ..., \lambda_7) = (1.1, 1.5, 2, 3, 5, 7, 10, 12)$ [27] which is enough for $n \leq 7$. In the absence of noises the differentiator provides for the FT exact estimations.

Equations (2) can be rewritten in the non-recursive form

$$\begin{aligned}
\dot{z}_0 &= -\tilde{\lambda}_n L^{\frac{1}{n+1}} \lfloor z_0 - f(t) \rceil^{\frac{n}{n+1}} + z_1, \\
\dot{z}_1 &= -\tilde{\lambda}_{n-1} L^{\frac{2}{n+1}} \lfloor z_0 - f(t) \rceil^{\frac{n-1}{n+1}} + z_2, \\
&\dots \\
\dot{z}_{n-1} &= -\tilde{\lambda}_1 L^{\frac{n}{n+1}} \lfloor z_0 - f(t) \rceil^{\frac{1}{n+1}} + z_n, \\
\dot{z}_n &= -\tilde{\lambda}_0 L \operatorname{sign}(z_0 - f(t)).
\end{aligned} \tag{3}$$

It is easy to see that $\tilde{\lambda}_0 = \lambda_0$, $\tilde{\lambda}_n = \lambda_n$, and $\tilde{\lambda}_j = \lambda_j \tilde{\lambda}_{j+1}^{j/(j+1)}$, $j = n-1, n-2, \dots, 1$.

Let the noise be absent, $\eta = 0$. Subtracting $f_0^{(i+1)}(t)$ from the both sides of the equation for $\dot{z}_i$ of (3), denoting $\sigma_i = (z_i - f_0^{(i)})/L$, $i = 0, ..., n$, $\vec{\sigma} = (\sigma_0, ..., \sigma_n)^T$, and using $f_0^{(n+1)}(t) \in [-L, L]$ obtain the FT-stable error dynamics [19]

$$\begin{aligned}
\dot{\sigma}_0 &= -\tilde{\lambda}_n \lfloor \sigma_0 \rceil^{\frac{n}{n+1}} + \sigma_1, \\
\dot{\sigma}_1 &= -\tilde{\lambda}_{n-1} \lfloor \sigma_0 \rceil^{\frac{n-1}{n+1}} + \sigma_2, \\
&\dots \\
\dot{\sigma}_{n-1} &= -\tilde{\lambda}_1 \lfloor \sigma_0 \rceil^{\frac{1}{n+1}} + \sigma_n, \\
\dot{\sigma}_n &\in -\tilde{\lambda}_0 \operatorname{sign} \sigma_0 + [-1, 1].
\end{aligned} \tag{4}$$

Here and further the DI is enlarged at the discontinuity points by the Filippov procedure [14] producing the Filippov DI. It is homogeneous with $\deg t = 1$, $\deg \sigma_i = n + 1 - i$ [19].

Notation. Assuming that the sequence $\vec{\lambda} = \{\lambda_j\}$, $j = 0, 1, ...$, produces the coefficients $\tilde{\lambda}_j$, denote (4) by the equality

$$\dot{\vec{\sigma}} \in \Delta_n(\sigma_0, \vec{\sigma}, \vec{\lambda}) + h_0,\ h_0 = (0, ..., 0, [-1, 1])^T. \tag{5}$$

with the first argument of the power function $\lfloor \cdot \rceil^{(\cdot)}$ singled out, and h_0 addressing the uncertainty of $f_0^{(n+1)}$. It is easy to see that (3) can be rewritten as $\dot{z} = L\Delta_n((z_0 - f)/L, z/L, \vec{\lambda})$.

Assumption 3 *The input $f(t)$ is sampled at the time instants t_k, $0 < t_{k+1} - t_k = \tau_k \le \tau$. The sampling intervals τ_k are bounded, $\tau_k \le \tau$, whereas $\tau > 0$ is unknown.*

Let the sampled difference $z_0(t) - f(t)$ be kept constant for $t \in [t_k, t_{k+1})$ producing

$$\dot{z} = L\Delta_n(\tfrac{1}{L}(z_0(t_k) - f(t_k)), \tfrac{1}{L}z, \vec{\lambda}),\ t \in [t_k, t_{k+1}). \tag{6}$$

Then, according to Theorem 8 from Appendix 8 for sampling time periods not exceeding $\tau > 0$ and the maximal possible sampling error $L\varepsilon \ge 0$ the differentiation accuracy [19,20]

$$\begin{aligned} &|z_i(t) - f_0^{(i)}(t)| \le \gamma_i L\rho^{n+1-i},\ i = 0,1,...,n, \\ &\rho = \max[\varepsilon^{1/(n+1)}, \tau] \end{aligned} \tag{7}$$

is ensured, where the constant numbers $\gamma_i \ge 1$ only depend on the parameters $\lambda_0, ..., \lambda_n$ of the differentiator. Accuracy (7) is kept for any $\varepsilon, \tau \ge 0, z(0), f_0, \eta$. The accuracy of differentiator (3) is formally included here as the continuous-sampling case $\tau = 0$.

It is proved that for constant L_0 any differentiator exact on noise-free inputs f_0, f_1 under Assumption 1 has the worst-case steady-state accuracy $\sup|z_i - f_0^{(i)}| = 2^{\frac{i}{n+1}} K_{n,i} L_0 \varepsilon^{\frac{n+1-i}{n+1}}$ for some f_0 and $\eta = f_1 - f_0$ [27]. Here $K_{n,i} \in [1, \pi/2]$ are the Kolmogorov constants [17,27], e.g. $K_{1,1} = \sqrt{2}$.

Correspondingly, a differentiator is called *asymptotically optimal* [18,19,27,28] if it has accuracy (7) for $\tau = 0$.

Remark 1 *Taking $z_0(t) - f(t_k)$ instead of $z_0(t_k) - f(t_k)$ in the differentiator* (6) *would create virtual measurements with unbounded sampling error, since $\dot{f}$ is not bounded under Assumptions 1, 2. It is easy to demonstrate the possible divergence of such a differentiator, for example taking $f(t) = t^2$, $n \ge 1$, $L = 2$, $\tau_k = \tau > 0$.*

3.2 Hybrid differentiator with variable L and $\varepsilon_L \ge 0$.

Suppose that $L(t) = L_0(t)$ is continuous, then under Assumption 2 differentiator (2) still *locally* converges in FT provided the initial errors satisfy $|z_j - f_0^{(j)}| \le \delta L$ for some $\delta > 0$, and δ, ε_L are small enough [22,27]. The corresponding accuracy still satisfies (7) for sufficiently small $\varepsilon, \varepsilon_L$ and τ. Divergence of differentiator (3) due to variable $L(t)$ is demonstrated in [24].

Introduce auxiliary functions φ_i, ϕ_i,

$$\begin{aligned} \phi_i(\tilde{\omega}) &= \lambda_{n-i}\lfloor\tilde{\omega}\rceil^{\frac{n-i}{n-i+1}} + \mu_{n-i}M\tilde{\omega}, \\ \varphi_i(t,\omega) &= L(t)\phi_i(\tfrac{1}{L(t)}\omega) \\ &= \lambda_{n-i}L(t)^{\frac{1}{n-i+1}}\lfloor\omega\rceil^{\frac{n-i}{n-i+1}} + \mu_{n-i}M\omega, \end{aligned} \tag{8}$$

where $\lambda_{n-i}, \mu_{n-i} > 0$, $i = 0,1,...,n$. Then under Assumptions 1, 2 the *hybrid* differentiator [24] features *global* fast convergence and has the form

$$\begin{aligned} \dot{z}_0 &= v_0 = -\varphi_0(t, z_0 - f(t)) + z_1, \\ \dot{z}_1 &= v_1 = -\varphi_1(t, z_1 - v_0) + z_2, \\ &\ldots \\ \dot{z}_n &= -\varphi_n(t, z_n - v_{n-1}). \end{aligned} \tag{9}$$

Its equivalent non-recursive form is

$$\begin{aligned} \dot{z}_0 &= -L(t)\bar{\phi}_0(\tfrac{1}{L(t)}[z_0 - f(t)]) + z_1, \\ \dot{z}_1 &= -L(t)\bar{\phi}_1(\tfrac{1}{L(t)}[z_0 - f(t)]) + z_2, \\ &\ldots \\ \dot{z}_n &= -L(t)\bar{\phi}_n(\tfrac{1}{L(t)}[z_0 - f(t)]), \\ \bar{\phi}_i(s) &= \phi_i(\phi_{i-1}(...(\phi_0(\tfrac{1}{L(t)}[z_0 - f(t)]))...)). \end{aligned} \tag{10}$$

Hybrid differentiator (8), (9) turns into the standard differentiator (2) for $M = 0$ and into the high-gain observer [3] if $\lambda_i = 0$ and $M >> 1$. That explains its name.

In the absence of sampling noises, $\varepsilon = 0$, and sufficiently small ε_L differentiator (9), (8) (and its nonrecursive form (10)) converges in FT for any initial conditions, provided the sequences $\vec{\lambda}, \vec{\mu}$ are properly chosen. Such double sequence $\{(\lambda_j, \mu_j)\}$ exists for any $\lambda_0 > 1, \mu_0 > 1$, and is valid for all n and $M \ge 0$ [24]. The sequence $\vec{\lambda} = \{\lambda_j\}$ is also valid for the "standard" differentiator (2). In particular, the sequence $(1.1,2)$, $(1.5,3)$, $(2,4)$, $(3,7)$, $(5,9)$, $(7,13)$, $(10,19)$, $(12,23)$, ... has been validated for $n \le 7$ [24,27].

Similarly to the standard differentiator (3) we rewrite (8), (10) as

$$\dot{z} = L(t)\Phi_n(\tfrac{1}{L(t)}[z_0 - f(t)], \tfrac{1}{L(t)}z, M, \vec{\lambda}, \vec{\mu}). \tag{11}$$

Obviously, $\Phi_n(\omega_0, \omega, 0, \vec{\lambda}, \vec{\mu}) = \Delta_n(\omega_0, \omega, \vec{\lambda})$.

Contrary to the simple non-recursive form (3) *of the standard differentiator* (2)*, the non-recursive form* (10) *is practically useless for $n > 1$.* Indeed, already the first-order differentiator (10) gets the complicated non-recursive form

$$\begin{aligned} &\dot{z}_0 = -\lambda_1 L^{\frac{1}{2}}\lfloor z_0 - f(t)\rceil^{\frac{1}{2}} - \mu_1 M(z_0 - f(t)) + z_1, \\ &\dot{z}_1 = -\lambda_0 L\,\mathrm{sign}(z_0 - f(t)) \\ &\quad -\mu_0\lambda_1 L^{\frac{1}{2}} M\lfloor z_0 - f(t)\rceil^{\frac{1}{2}} - \mu_0\mu_1 M^2(z_0 - f(t)). \end{aligned} \tag{12}$$

The Lyapunov-method convergence proof for (12) has been recently published in [10].

The dynamics of the normalized error $\vec{\sigma}$ corresponding to (11) are not homogeneous, but feature homogeneity in bilimit [1] with a negative approximating homegeneity degree at zero and the zero homogeneity degree at infinity [24].

Note that the approximately linear dynamics of large $\vec{\sigma}$ can lose their stability for large enough τ, causing the instability of the differentiator itself (Fig. 7). Large noises do not destroy the dynamics stability, but the accuracy asymptotics change (Section 6.2). Thus, under Assumptions 1, 2, 3 differentiator (9),(8) with discrete measurements provides for the same accuracy (7) *for sufficiently small $\varepsilon_L, \varepsilon, \tau$* [24].

4 Discretization of SM differentiators

In reality the described differentiators are realized by means of computers. This turns a real-time differentiator into a discrete dynamic system handling the noisy input $f(t) = f_0(t) + \eta(t)$ produced by the continuous-time DI $f_0^{(n+1)} \in L_0[-1,1]$. The SM-based system (3) or (10) is to be numerically integrated. *The aim of this paper is to propose and study the corresponding integration schemes.*

Assumption 4 *Let t_k be the sampling instants. The integration steps take place at the discrete time instants $t_{k,j}$, $j = 0,...,l_k$, $t_{k,0} = t_k$, $t_{k,l_k} = t_{k+1} = t_{k+1,0}$. Thus, all sampling* *instants are also the points of the integration subdivision. It is also assumed that the integration steps are bounded,* $0 < t_{k,j+1} - t_{k,j} = \underline{\tau}_{k,j} \le \underline{\tau}$.

Assumptions 3, 4 imply that $\underline{\tau} \le \tau$. The authors took 100 and more equal Euler integration steps between sampling instants, but for $n > 1$ the accuracy remained much worse than the predicted accuracy (7) (Section 6.1, Fig. 3). The question why the standard accuracy is not restored in spite of small integration steps between the measurements remained unsolved till the recent conference paper [6].

In short, the answer is that the number of the integration steps over each sampling interval is to be of the order $\tau^{-(n-1)}$, which becomes very large for $n > 1$ and $\tau << 1$.

4.1 *Discretization of homogeneous differentiators*

This subsection extends the results [30] to the case when each sampling interval contains a number of integration steps. We also significantly generalize the method of homogeneous discretization proposed in [30].

Consider the standard differentiator (2) or (3), which is represented as $\dot{z} = L\Delta_n((z_0 - f)/L, z/L, \vec{\lambda})$. In this subsection the function L is constant, and $L_0 = L$, $\varepsilon_L = 0$ are assumed without loss of generality.

The Euler discretization of (3) takes the form

$$\begin{aligned} &z(t_{k,j+1}) = z(t_{k,j}) + L\Delta_n(\tfrac{z_0(t_k)-f(t_k)}{L}, \tfrac{z(t_{k,j})}{L}, \vec{\lambda})\underline{\tau}_{k,j}, \\ &j = 0,...,l_k - 1, t_{k+1} = t_{k+1,0} = t_{k,l_k}, k = 0,1,2,... . \end{aligned} \tag{13}$$

Theorem 2 *Consider the standard homogeneous differentiator* (2) *under assumptions 1-4. Let* $L > 0$ *be constant,* $\varepsilon_L = 0$, *and the **integration** steps be equal,* $t_{k,j+1} - t_{k,j} = \underline{\tau}_{k,j} = \underline{\tau}$. *Also suppose that the derivatives* $f_0^{(i)}$ *of the orders* $2,3,...,n$ *are bounded:* $|f_0^{(i)}|/L \le D_i$, $D_{n+1} = 1$. *Then there exist such constants* $\gamma_i > 0$ *that the inequalities*

$$\begin{aligned} &|z_0(t_{k,j}) - f_0(t_{k,j})| \le \gamma_0 L\rho^{n+1};\ \rho = \max[\varepsilon^{\frac{1}{n+1}}, \tau] \\ &|z_i(t_{k,j}) - f_0^{(i)}(t_{k,j})| \le \gamma_i L\rho^{n+1-i} + iL\underline{\tau}D_{i+1}, i = 1,...,n, \end{aligned} \tag{14}$$

hold after a FT transient for any input and initial values of the discrete differentiator (13). *Coefficients* $\gamma_i > 0$ *are only defined by the parameters* $\lambda_0,...,\lambda_n$ *of the differentiator.*

Hence, asymptotics (14) known for coinciding integration and sampling steps, $l_k = 1$, with constant sampling intervals, $\tau_k = \underline{\tau} = \tau$ [30], remain true for *variable* sampling intervals τ_k, provided the Euler integration steps $\underline{\tau}_{k,j}$ are *equal*.

Theorem 3 *Under the conditions of Theorem 2 let also the integration steps be variable and uniformly bounded,* $\underline{\tau} \le \underline{\tau}_M$. *Then for some constants* $\gamma_i > 0$ *the inequalities*

$$\begin{aligned} &|z_i(t_{k,j}) - f_0^{(i)}(t_{k,j})| \le \gamma_i L\rho^{n+1-i}, i = 0,1,...,n, \\ &\rho = \max[\varepsilon^{1/(n+1)}, \underline{\tau}^{1/n}, \tau] \end{aligned} \tag{15}$$

hold after a FT transient for any τ *and* $\underline{\tau} \le \min[\tau, \underline{\tau}_M]$. *Note that coefficients* γ_i *depend on* $\lambda_0,...,\lambda_n$, $D_2,...,D_n$ *and* $\underline{\tau}_M$.

Fixing $\underline{\tau}_M = 1$ get that the standard asymptotics (7) are only restored for $\underline{\tau} = O(\tau^n)$. Also the boundedness requirement for derivatives $f_0^{(i)}$, $i = 2,...,n$, is restrictive. The following discretization removes all these limitations.

Homogeneous Discrete Differentiator. The proposed discrete differentiator contains correction terms $H_n, \hat{H}_n \in \mathbb{R}^{n+1}$,

$$\begin{aligned} &z(t_{k,j+1}) = z(t_{k,j}) + L\Delta_n(\tfrac{z_0(t_k)-f(t_k)}{L}, \tfrac{z(t_{k,j})}{L}, \vec{\lambda})\underline{\tau}_{k,j} \\ &+H_n(z(t_{k,j}), \underline{\tau}_{k,j})\underline{\tau}_{k,j}^2 + L\hat{H}_n(\tfrac{z_0(t_k)-f(t_k)}{L}, \underline{\tau}_{k,j})\underline{\tau}_{k,j}^{1+\chi}, \\ &0 < \chi \le 1,\ j = 0,...,l_k - 1, \end{aligned} \tag{16}$$

Let $\omega, s \in \mathbb{R}$. The vector H_n contains Taylor-like terms,

$$\begin{aligned} &H_{n,i}(z,\omega)\omega^2 = \tfrac{z_{i+2}}{2!}\omega^2 + \tfrac{z_{i+3}}{3!}\omega^3 + ... + \tfrac{z_n}{(n-i)!}\omega^{n-i}, \\ &\qquad\qquad i = 0,...,n-2, \\ &H_{n,n-1}(z,\omega) = H_{n,n}(z,\omega) = 0. \end{aligned} \tag{17}$$

The vector correction term $\hat{H}_n(s,\omega)$ is assumed bounded in a vicinity of $(s,\omega) = (0,0)$, and for $\deg s = n+1$, $\deg \omega = 1$ satisfies the homogeneity conditions

$$\begin{aligned} &\deg[\hat{H}_{n,i}(s,\omega)\omega^{1+\chi}] = n - i + 1,\ i = 0,1,...,n-1, \\ &\hat{H}_{n,n}(s,\omega) = 0. \end{aligned} \tag{18}$$

Terms $H_n, \hat{H}_n$ grant homogeneity properties to the discrete error dynamics. The term H_n *is required, but only appears for* $n > 1$. The dicretization [30] corresponds to the case $\hat{H}_n = 0$, $l_k = 1$, $\underline{\tau}_{k,0} = \tau_k$. Note that (16) can be also rewritten in the recursive form for $\hat{H}_n = 0$ (see (26) below).

Exact discretization. Rewrite (3) in the form

$$\begin{aligned} &\dot{z} = W(z_0 - f(t)) + J_{n+1}z, \\ &W_i(s) = -\tilde{\lambda}_{n-i}L^{\frac{i+1}{n+1}}\lfloor s\rceil^{\frac{n-i}{n+1}},\ i = 0,...,n, \end{aligned} \tag{19}$$

where J_{n+1} is the $(n+1)\times(n+1)$ Jordan block with the zero diagonal. Under Assumptions 1-3 its exact discretization is

$$z(t_{k+1}) = e^{J_{n+1}\tau_k}z(t_k) + \left[\int_0^{\tau_k} e^{J_{n+1}\omega}d\omega\right]W(z_0(t_k) - f(t_k)). \tag{20}$$

One can see that (20) is a particular case of (16)-(18) for $l_k = 1$, $\underline{\tau}_{k,0} = \tau_k$, $\chi = 1$, and

$$\begin{aligned} &H_n(z,\omega)\omega^2 = e^{J_{n+1}\omega}z - z - J_{n+1}z\omega, \\ &\hat{H}_{n,i}(s,\omega)\omega^2 = \\ &\quad -\tfrac{\tilde{\lambda}_{n-i-1}}{2!}\lfloor s\rceil^{\frac{n-i-1}{n+1}}\omega^2 - ... - \tfrac{\tilde{\lambda}_0}{(n-i+1)!}\lfloor s\rceil^0\omega^{n-i+1}. \end{aligned} \tag{21}$$

Theorem 4 *Under Assumptions 1-4 and for any* $\underline{\tau}, \tau > 0$, $\underline{\tau} \le \tau$, $\varepsilon_L = 0$, $L = const$, *differentiator* (16) *in FT provides for the accuracy*

$$\begin{aligned} &|z_i(t_{k,j}) - f_0^{(i)}(t_{k,j})| \le \gamma_i L\rho^{n+1-i},\ i = 0,1,...,n, \\ &\rho = \max[\varepsilon^{1/(n+1)}, \tau],\ \ j = 1,...,l_k, \end{aligned} \tag{22}$$

for some constants $\gamma_i > 0$ *independent of the function* f_0 *and the choice of the sampling intervals and integration steps.*

Thus, discrete differentiator (16) completely reclaims the accuracy asymptotics (7) of its continuous-time analogue. This result has been obtained in [30] for $\hat{H}_n = 0$ and the coinciding integration and sampling intervals. The term $\hat{H}_n$ only influences the coefficients γ_i. The simulation (Section 6.1) shows that additional integration steps and $\hat{H}_n$ from (21) do not cause any noticeable accuracy change.

4.2 Discrete hybrid differentiator with variable L, $\varepsilon_L \ge 0$.

Results [6,30] are extended here to differentiators (9), (8).

Let $L(t)$ be variable, and $|\dot{L}|/L \le M$ hold for some M. Then under Assumptions 1, 2, 3 above schemes make sense and have similar accuracies. The Euler-integration-based discrete differentiator corresponding to the variable-gain hybrid differentiator (10) takes the form

$$\begin{aligned} &z(t_{k,j+1}) = z(t_{k,j}) + \\ &\qquad L(t_k)\Phi_n\big(\tfrac{z_0(t_k)-f(t_k)}{L(t_k)}, \tfrac{z(t_{k,j})}{L(t_k)}, M, \vec{\lambda}, \vec{\mu}\big)\underline{\tau}_{k,j}, \qquad (23) \\ &j = 0,...,l_k-1,\ t_{k+1} = t_{k+1,0} = t_{k,l_k},\ k = 0,1,2,... . \end{aligned}$$

By formally substituting $M = 0$ in (23) obtain the discrete scheme (13) for differentiator (2), but with variable L, i.e.

$$z(t_{k,j+1}) = z(t_{k,j}) + L(t_k)\Delta_n\big(\tfrac{z_0(t_k)-f(t_k)}{L(t_k)}, \tfrac{z(t_{k,j})}{L(t_k)}, \vec{\lambda}\big)\underline{\tau}_{k,j}. \qquad (24)$$

Under Assumption 2 with $M > 0$ scheme (24) is only reliable for sufficiently small initial errors.

Theorem 5 *Theorems 2 and 3 remain true for the case when $L(t)$ is variable with the following changes:*

(1) if scheme (24) is applied in spite of $M > 0$ the noise amplitudes $\varepsilon, \varepsilon_L$, the maximal sampling interval τ and the initial error $\vec{\sigma}(t_0)$ are to be small enough;

(2) in the case of the hybrid differentiator (23) with $M > 0$ the noise amplitudes $\varepsilon, \varepsilon_L$, and the maximal sampling interval τ are to be small enough, but there is no restriction on the initial error $\vec{\sigma}(t_0)$.

Also here proper discretization allows to restore the accuracy (7). The term $\hat{H}_n$ of (16)-(18) is not applicable here. The modified discrete hybrid differentiator (23) turns to be

$$\begin{aligned} &z(t_{k,j+1}) = z(t_{k,j}) + \\ &L(t_k)\Phi_n\big(\tfrac{z_0(t_k)-f(t_k)}{L(t_k)}, \tfrac{z(t_{k,j})}{L(t_k)}, M, \vec{\lambda}, \vec{\mu}\big)\underline{\tau}_{k,j} \qquad (25) \\ &\qquad + H_n(z(t_{k,j}), \underline{\tau}_{k,j})\underline{\tau}_{k,j}^2, \end{aligned}$$

where H_n is defined in (17).

In practice it is more convenient to use the equivalent recursive form using functions φ_i, v_i from (8), (9),

$$\begin{aligned} &z_0(t_{k,j+1}) = z_0(t_{k,j}) + \underline{\tau}_{k,j} v_0(t_{k,j}) + H_{n,0}(z(t_{k,j}), \underline{\tau}_{k,j})\underline{\tau}_{k,j}^2, \\ &\qquad v_0(t_{k,j}) = -\varphi_0(t_k, z_0(t_k) - f(t_k)) + z_1(t_{k,j}), \\ &z_1(t_{k,j+1}) = z_1(t_{k,j}) + \underline{\tau}_{k,j} v_1(t_{k,j}) + H_{n,1}(z(t_{k,j}), \underline{\tau}_{k,j})\underline{\tau}_{k,j}^2, \\ &\qquad v_1(t_{k,j}) = -\varphi_1(t_k, z_1(t_{k,j}) - v_0(t_{k,j})) + z_2(t_{k,j}), \\ &... \\ &z_n(t_{k,j+1}) = z_n(t_{k,j}) + \underline{\tau}_{k,j} v_n(t_{k,j}) + H_{n,n}(z(t_{k,j}), \underline{\tau}_{k,j})\underline{\tau}_{k,j}^2; \\ &\qquad v_n(t_{k,j}) = -\varphi_n(t_k, z_n(t_{k,j}) - v_{n-1}(t_{k,j})); \\ &j = 0,...,l_k-1,\ t_{k+1} = t_{k+1,0} = t_{k,l_k},\ k = 0,1,2,... . \end{aligned} \qquad (26)$$

Formally substituting $M = 0$ turns (26) into the recursive form of (24). Also here the Taylor terms H_n do not appear for $n = 0,1$, since $H_{n,n} = H_{n,n-1} = 0$.

Theorem 6 *Under assumptions 1, 2, 3 there exist such constants $\gamma_i > 0$, $i = 0,1,...,n$, that for any sufficiently small maximal sampling step τ and noise magnitudes $\varepsilon, \varepsilon_L$ independently of the input function f_0 and the choice of the sampling intervals and integration steps the inequalities (22) hold after a FT transient of the hybrid differentiator (25).*

Remark 2 *Calculating $z(t_{k+1})$ only requires the values of $f(t_k)$, $z(t_k)$ and t_{k+1}. Thus, one can estimate the derivatives at **any** time $t \in (t_k, t_k+\tau]$ by applying the corresponding discrete scheme up to the time t and formally considering t as the virtual sampling time t_{k+1}. It preserves the precision stated in Theorems 2-6, provided $t_k, f(t_k), z(t_k)$ correspond to the differentiator steady state, and actually becomes a **prediction**, if t is still in the future.*

5 Differentiation of event-triggered sensor outputs

All the differentiation results presented in Sections 3-4 required Assumption 3 that the sampling intervals are bounded by τ, though the bound τ itself can be unknown. In some important practical cases that assumption does not hold.

Let the sensor yielding the input signal $f(t)$ have its own logic preventing new measurements if the signal has not significantly changed. The reason can be saving the bounded information pass band or the sensor structure. For example, a tachometer differentiates the rotation angle measured using a photo-diode detecting the passing-it slot of a rotating disk. Thus, the sampling time intervals become unbounded when the disk is slowing down.

Surprisingly, large sampling intervals due to slowly changing inputs can destroy the filter accuracy and even lead to instability, if the filter contains terms of non-negative homogeneity degrees (for example for linear filters) [21]. In particular, differentiators (23), (25) can lose stability (see simulation in Section 6.3). A simple strategy proposed below removes such danger.

Assumption 3 is removed in this section. The following assumption is used instead of Assumption 1b.

Assumption 5 *At no moment between the measurements the actual value of the unknown smooth signal $f_0(t)$ differs from the last measured value by more than $\varepsilon_T L(t)$, $\varepsilon_T > 0$.*

For generality the value ε_T is assumed unknown. Note that Assumption 5 also does not exclude the existence of measurement noises $\eta(t)$ with bounded ratio η/L.

A constant measurement error threshold is included in the assumption, if L is constant or separated from zero. Indeed, one can always take new function $\tilde{L} = L + h$, $h > 0$. The following is the alternative assumption in the case one considers not reasonable that a sensor is "aware" of the value $L(t)$.

Assumption 6 *The actual value of the unknown smooth signal $f_0(t)$ never differs from the last measured value by more than ε_T, $\varepsilon_T > 0$. $L(t)$ is separated from zero, $L(t) \ge L_m > 0$.*

Assumptions 5, 6 allow taking *a virtual measurement* at any moment. One simply once more takes the last measured value, since such "measurement" does not introduce error exceeding $L(t)\varepsilon_T$ (Assumption 5) or ε_T (Assumption 6).

Suppose that a virtual measurement is performed at each time $t \in [t_k, t_{k+1})$ ($t_{k+1} = \infty$ is allowed), when the time since the last real/virtual sampling passes the value $\tau_{T,k} > 0$, and the real measurement does not occur.

The following theorem is a direct corollary of Theorems 2-6.

Theorem 7 *All theorems 2-6 remain true under Assumptions 1a, 2, 4, 5 for $\varepsilon = \varepsilon_T$ and $\tau = \tau_{T,k} = const$. Moreover, if the threshold ε_T is known, taking variable $\tau_{T,k} \le \tau = C_T \varepsilon_T^{\frac{1}{n+1}}$ for some constant $C_T > 0$ provides for the accuracy (22) of the discrete differentiator (25). Similarly under Assumptions 1a, 2, 4, 6 one gets accuracy (22) for $\tau_{T,k} \le C_T(\frac{\varepsilon_T}{L(t_k)})^{\frac{1}{n+1}}$, $\tau = C_T(\frac{\varepsilon_T}{L_m})^{\frac{1}{n+1}}$, $\varepsilon = \frac{\varepsilon_T}{L_m}$.*

The theorem implies that a valid fault-proof strategy is simply to choose the least practically-possible τ_T.

6 Numeric experiments

The presented results are obtained by fitting suitable discrete homogeneous dynamic models to complicated *nonhomogeneous* processes (see the proofs in appendices). Being true for all possible inputs the resulting estimations are inevitably very rough. In the following we study the proposed discretizations numerically.

The suggested parameters $\vec{\lambda} = \{1.1, 1.5, 2, 3, 5, 7, 10, 12, ...\}$ [24,27] correspond to the parameters $\tilde{\lambda}_i$ of the differentiator (2) in its non-recursive form (3) for $n \leq 7$ (Fig. 1). Recall that the hybrid differentiator always has the recursive form (8), (9) with the same $\vec{\lambda}$ and $\vec{\mu} = \{2, 3, 4, 7, 9, 13, 19, 23, ...\}$.

n	$\tilde{\lambda}_0$	$\tilde{\lambda}_1$	$\tilde{\lambda}_2$	$\tilde{\lambda}_3$	$\tilde{\lambda}_4$	$\tilde{\lambda}_5$	$\tilde{\lambda}_6$	$\tilde{\lambda}_7$
0	1.1							
1	1.1	1.5						
2	1.1	2.12	2					
3	1.1	3.06	4.16	3				
4	1.1	4.57	9.30	10.03	5			
5	1.1	6.75	20.26	32.24	23.72	7		
6	1.1	9.91	43.65	101.96	110.08	47.69	10	
7	1.1	14.13	88.78	295.74	455.40	281.37	84.14	12

Fig. 1. Optional parameters $\tilde{\lambda}_0, \tilde{\lambda}_1, ..., \tilde{\lambda}_n$ of differentiator (3).

The following software/computer-based accuracy restrictions are crucially important in the numerical study.

Digital accuracy restrictions. The double-precision computer number has 15 meaningful decimal digits corresponding to the input noise of the magnitude $5 \cdot 10^{-16}$ for signals close to 1. In particular, in that case the accuracy $\sup|z_0 - f_0|$ is not better than $5 \cdot 10^{-16}$, and the 5th-order-derivative accuracy of **any** 5th-order differentiator is expected to be not better than $(\pi/2) \cdot 2^{5/6}(5 \cdot 10^{-16})^{1/6} \approx 0.01$ for $L = 1$ [27].

Notation. Introduce the notation *EDD* for the Euler discretization scheme (13) of the differentiator (3) and *HDD* for homogeneous discrete differentiator (16) with the additional Taylor-like term H_n of the form (17), but with $\hat{H}_n = 0$. The homogeneous discrete differentiator (20) is denoted as *exact HDD* and corresponds to (16) with $\hat{H}_n$ in the form (21).

Correspondingly *EDHD* denotes the Euler discretization scheme (23) of the hybrid differentiator, and *HDHD* denotes the scheme (25), i.e. (23) with the additional term H_n.

6.1 Performance in the absence of noises

Taking into account the theoretical asymptotics (22) and the above digital accuracy restrictions it is convenient to choose an input signal $f_0(t)$ of the magnitude close to 1 and featuring $|f_0^{(n+1)}| \leq 1$. Choose the input $f(t) = f_0(t) + \eta(t)$, $|\eta(t)| \leq \varepsilon$, where

$$f_0(t) = 0.5\cos(t) + \sin(0.5t), \qquad (27)$$

and assign $L = L_0 = 1$ for all differentiation orders. Let $\varepsilon = 0$ to get the best possible digital discretization accuracy. Choose the differentiation order $n = 5$ and zero initial differentiator conditions.

Hybrid differentiator (11) features the same dynamics as differentiator (5) *for small enough errors, noises and sampling intervals*. Thus the above digital restrictions leave only a very narrow range of τ available (see Fig. 4a). It is natural, therefore, to start with the "standard" differentiator (5) to study the accuracy of schemes in the absence of noises.

First consider the most widespread case of equal sampling steps and substeps. That case corresponds to Theorem 2. Correspondingly τ is the constant sampling step, while $\underline{\tau} = \tau/N$ is the constant Euler integration substep.

Denote $\tilde{\sigma}_i = z_i - f_0^{(i)}$, $|\tilde{\sigma}|_n = (|\tilde{\sigma}_0|, ..., |\tilde{\sigma}_n|)$. The convergence graphs for $t \in [0, 20]$ appear in Fig. 2. List the corresponding accuracies.

The accuracy of EDD with $N = 50$, $\tau = 0.01$, calculated over the steady state interval $t \in [10, 30]$ is provided by the component-wise inequality $|\tilde{\sigma}|_5 \leq$
$(2.0 \cdot 10^{-9}, 5.1 \cdot 10^{-5}, 1.3 \cdot 10^{-4}, 8.5 \cdot 10^{-4}, 0.013, 0.12)$,
whereas the accuracy of HDD for $N = 1$, $\underline{\tau} = \tau = 0.01$ (Fig. 2), is $|\tilde{\sigma}|_5 \leq$
$(3.7 \cdot 10^{-9}, 4.3 \cdot 10^{-7}, 3.2 \cdot 10^{-5}, 1.0 \cdot 10^{-3}, 0.017, 0.15)$.
The accuracy of the exact HDD differs from the HDD only in the 5th meaningful digit of each component and is omitted.

The accuracy of the EDD with $N = 1$, $\underline{\tau} = \tau = 0.0001$, for $t \in [10, 30]$ (Fig. 2) is $|\tilde{\sigma}|_5 \leq$
$(6.7 \cdot 10^{-16}, 3.75 \cdot 10^{-5}, 5.9 \cdot 10^{-5}, 8.4 \cdot 10^{-5}, 1.6 \cdot 10^{-4}, 0.13)$,
whereas the accuracy of the HDD and the exact HDD is $|\tilde{\sigma}|_5 \leq$
$(4.4 \cdot 10^{-16}, 8.6 \cdot 10^{-13}, 7.2 \cdot 10^{-10}, 3.4 \cdot 10^{-7}, 8.5 \cdot 10^{-5}, 0.13)$.

The graphs of z_i for all the schemes do not visually differ for $\tau = 0.0001$. For the comparison, in Fig. 2 we also demonstrate the simple divided-difference estimation of $f_0^{(5)}$ exploding due to the computer round-up errors.

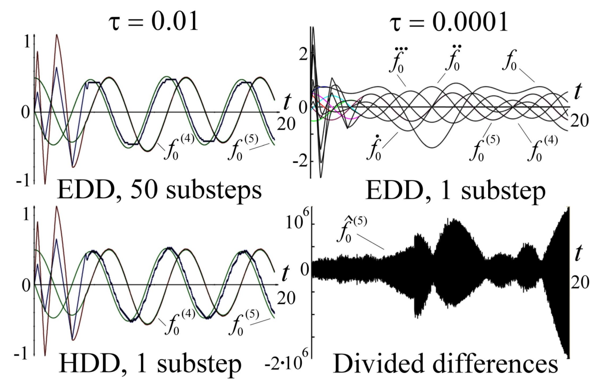

Fig. 2. Performance without noise. Left: estimations of $f_0^{(4)}$ and $f_0^{(5)}$ by the 5th-order EDD with $N = 50$, $\underline{\tau} = \tau/50$, and HDD for $\tau = 0.01$ and input (27). Right: convergence of the estimations by EDD/HDD for $\tau = 0.0001$, the divided-difference explosion.

According to Theorems 2, 4 the accuracy asymptotics of HDD, exact HDD for $N = 1$ and EDD for $N = O(\tau^{1-n}) = O(\tau^{-4})$ are to be the same up to possibly different coefficients. Fig. 3a shows that the accuracies of HDD and exact HDD *coincide* at least for the input (27). The direct lines in the graph have the slopes 6.02, 5.02, 4.03, 3.02, 1.99, 0.90 which very well fit the theoretical asymptotics.

Note that the *negation* of the term (21) in (16) causes some accuracy improvement (up to 30%, not shown). Another particular choice of the terms $\hat{H}_n$ (18) has been quite recently independently proved and shown to improve the accuracy-asymptotics' coefficients in simulation for equal sampling steps and absent additional integration substeps [16].

Numeric experiments reveal *surprising features* of the EDD for different values of N and $\tau \in [0.0001, 0.1]$. The logarithmic plot in Fig. 3b shows that there exists a direct bifurcation line depending on N, and corresponding to the direct proportionality of the derivative-estimation accuracy to the sampling step τ.

Roughly speaking, above the line the accuracies are the same as of the HDD, whereas the accuracy lines for deriva-

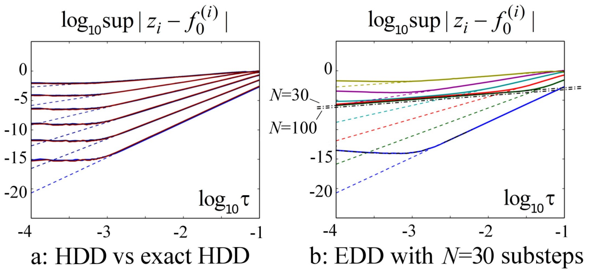

Fig. 3. Logarithmic graphs of the 5th-order differentiation accuracies. The graphs correspond to the derivative orders 0, 1, 2, 3, 4, 5 from the bottom to the top. Integration and sampling steps are constant, $\underline{\tau} = \tau/N$. a: $N = 1$. Accuracies of HDD (in red) and exact HDD (in blue) are practically identical. b: EDD with $N = 30$, the bifurcation lines for $N = 30, 100$ are shown.

tives 2,3,4 break at the bifurcation line and follow it to the left of their intersections with it. Accuracies of the last 5th derivative and the tracking accuracy of the 0th derivative f_0 remain roughly the same as those of the HDD.

The bifurcation line moves down when N grows from 1 to infinity. That motion slows down for larger N. The lines for $N = 30$ and $N = 100$ are shown in the graph (Fig. 3b). The line corresponding to $N = 50$ is between them and cannot be shown. Obviously there is no much difference between the accuracies for $N = 30, 50, 100$.

According to Theorems 2-4 there exists such $\Gamma_n > 0$ that under the listed assumptions the inequality $\underline{\tau} \le \Gamma_n \tau^n$ ensures asymptotics (22) for all inputs, all sampling and integration subdivision strategies.

Solving the equation $\tau_*/N = \Gamma_b \tau_*^n$, $n = 5$, for Γ_b at the intersection point $\tau = \tau_*$ of the bifurcation line and the accuracy line for $z_1 - \dot{f}_0$ obtain that the HDD asymptotics of EDD hold for $\tau \ge \tau_*$, i.e. while $\underline{\tau} = \tau/N \le \Gamma_b \tau^5$ holds. Calculating Γ_b for $N = 30, 50, 100$ obtain $\Gamma_b \approx 5000$. Naturally $\Gamma_5 \le 5000$ is to hold.

The case of variable sampling and integration steps. Consider the 5th-order **hybrid differentiator** (11) with the same $\vec{\lambda}, \vec{\mu}$, as mentioned above, and $L = M = 1$. The initial values $(z_0(0), ..., z_5(0)) = (100, -100, 100, ..., -100)$ are taken to demonstrate the fast differentiator convergence. The accuracy $|\tilde{\sigma}|_5 \le$
$(3.3 \cdot 10^{-16}, 7.3 \cdot 10^{-13}, 6.9 \cdot 10^{-10}, 3.3 \cdot 10^{-7}, 8.4 \cdot 10^{-5}, 0.12)$.
is got by the corresponding HDHD for $\tau = 10^{-4}, t \ge 13.2$.

One expects (Theorem 5) that for sufficiently large τ the hybrid differentiator (23) is not stable, for smaller τ the accuracies obey the standard HDD asymptotics (7), $|z_i(t) - f_0^{(i)}(t)| \le \gamma_i \tau^{6-i}$. Those asymptotics are once more destroyed when $\underline{\tau}$ becomes too large compared with τ^5 (Theorem 5, accuracy (15)), further also those asymptotics are destroyed by the digital saturation for even smaller τ.

The hybrid differentiator indeed diverges in the simulation for $\tau > 0.06$ and Fig. 3 implies that the digital saturation takes place for $\tau \le 0.001$. Also further see the HDHD performance in Fig. 6 for small τ and $n = 3$.

As we see, fixing a maximal sampling step τ and gradually reducing the maximal integration step $\underline{\tau}$ is not realistic, since the HDD accuracy reclamation requires $\underline{\tau} = O(\tau^5)$. Instead fix the maximal integration step $\underline{\tau} = 0.0001$ and gradually increase τ starting from $\tau = \underline{\tau}$, while calculating the corresponding accuracies $\sup|z_i - f_0^{(i)}|$ over the steady-state time interval $t \in [14, 16]$.

The random sampling intervals τ_k are taken uniformly distributed in the range $[10^{-4}, \tau]$, whereas τ remains constant during each run, $\tau \in [10^{-4}, 0.05]$. Also the integration steps $\underline{\tau}_{kj}$ are uniformly distributed in the range $[10^{-6}, 10^{-4}]$.

Note that this Monte-Carlo experiment strategy completely excludes the case $\tau_j = \tau$, $\underline{\tau}_{kj} = \tau/N$, considered above, due to its obvious "improbability".

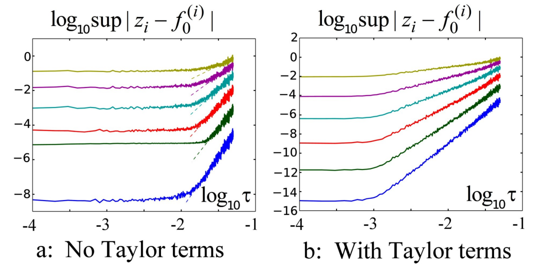

Fig. 4. Logarithmic graphs of the 5th-order differentiation accuracies for $\underline{\tau} = 0.0001$: a: EDHD differentiator (23), b: HDHD (25). The lines correspond to the derivative orders 0, 1, 2, 3, 4, 5 from the bottom to the top. Integration and sampling steps are variable.

The standard continuous-time asymptotics (22) are only kept for $\tau \in [0.03, 0.06]$ (Fig. 4a). The inequality $\tau \ge 0.03$ corresponds to $\underline{\tau} \le \Gamma_v \tau^5$ for $\Gamma_v \approx 4000$. Thus, the above universal constant Γ_5 satisfies $\Gamma_5 \le 4000$ which is consistent with the estimation $\Gamma_5 \le 5000$ obtained from Fig. 3.

Thus, in order to get asymptotics (22) one needs $\underline{\tau} \le 4 \cdot 10^{-7}$ for $\tau = 0.01$, and $\underline{\tau} \le 1.3 \cdot 10^{-10}$ for $\tau = 0.002$.

It is also seen from the graphs that $\sup|z_5 - f_0^{(5)}|$ stabilizes at about 0.1 which is ten times larger than the hypothetical best possible accuracy 0.01. The tracking accuracy stabilizes at $|z_0 - f_0| \le 6 \cdot 10^{-9}$, which is much worse than the best possible digital error $5 \cdot 10^{-16}$.

Consider now the discrete hybrid differentiator (26) with additional Taylor-like terms. One sees from Fig. 4b that it features the ideal continuous-time asymptotics for $\tau \in [0.001, 0.02]$. At $\tau = 0.001$ the tracking accuracy stabilizes at almost the best possible computer precision 10^{-15}. At the same time the 5th-order derivative estimation accuracy is about 0.02, which is close to the expected best possible value. The graph slopes calculated over the interval $\log_{10}\tau \in [-2, -2.5]$ are $5.9, 4.8, 4.0, 3.0, 2.0, 1.0$ from the bottom to the top (Fig. 4) and fit the theory very well.

Hence, the simulation shows that *variable* integration steps significantly destroy the EDD and EHDD asymptotics in comparison with the HDD and the HDHD respectively. It also shows that additional intermediate integration steps practically do not affect the HDD or HDHD accuracy (compare Figs. 3a, 4b).

6.2 Effect of noises

The choice of sampling steps and the integration subdivision have minor influence on the differentiator accuracy in the presence of large, usual and reasonably small noises $\eta, |\eta| \le \varepsilon$. Indeed, accuracies (15) are the functions of $\rho = \max[\varepsilon^{1/(n+1)}, \underline{\tau}^{1/n}, \tau]$. Our experiments in the presence of noises demonstrate that EDD and HDD, as well as EDHD and HDHD, provide for the same accuracies up to 3 meaningful digits.

Performance of EDDs/HDDs in the presence of noises has been well studied. Thus we concentrate on the hybrid differentiators. Their fast convergence and insensitivity to changing L has a price involved.

The hybrid differentiators EDHD/HDHD feature the nonlinear dynamics (4) of the EDD/HDD for small errors corresponding to $\vec{\mu} = 0$. For larger errors the dynamics are quasi-linear almost as if $\vec{\lambda} = 0$ were true. This quasi-linearity provides for the fast exponential convergence, but also for the overregulation, the steady-state error proportional to ε for larger ε and the sensitivity to large sampling intervals.

Fix $\underline{\tau} = \tau = 0.0001$. The value $M = 1$ is found to cause rather high sensitivity to noises. Performance of the EDHD/HDHD in the presence of different noises for $M = 0.2$, $z(0) = 0$ is presented in Fig. 5.

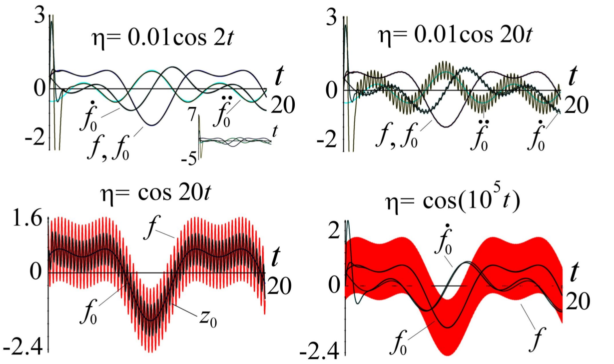

Fig. 5. Performance of the HDHD/EDHD with $M = 0.2$ in the presence of different noises η for $\tau = 10^{-4}$. Upper graphs are cut from above and from below. The shrinked complete graph is added in the case $\eta = 0.01\cos(2t)$.

The noise $\eta = 0.01\cos(2t)$ is practically exactly differentiated by EDHD, and the corresponding accuracy is covered by the Kolmogorov-like worst-case steady-state accuracy

$$\sup|z_i - f_0^{(i)}| \in 2^{\frac{i}{n+1}}[1, \pi/2]L\varepsilon^{\frac{n+1-i}{n+1}}, \tag{28}$$

where $n = 5$ [27] (Section 3.1). The resulting accuracy is $|\tilde{\sigma}|_5 \leq (0.01, 0.02, 0.04, 0.08, 0.16, 0.33)$. The same accuracy is obtained for $M = 1$ and $M = 0$ (i.e. by EDD/HDD).

The noise $\eta = 0.01\cos(20t)$ has a large 6th derivative, and while the accuracy (22) remains in charge, the obtained accuracy $|\tilde{\sigma}|_5 \leq (0.099, 0.098, 0.48, 1.20, 1.67, 1.25)$ is not covered by (28). Note that the accuracy $|\tilde{\sigma}|_5 \leq (0.015, 0.24, 2.19, 10.2, 32.6, 65.3)$ is obtained for $M = 1$, and is clearly produced by the quasi-linear large-scale dynamics. For the comparison, the EDD corresponding to $M = 0$ provides for the accuracy $|\tilde{\sigma}|_5 \leq (0.011, 0.10, 0.47, 1.10, 1.29, 0.82)$.

The noise $\eta = \cos(20t)$ is certainly not covered by (28), and is very challenging for the EDHD. The corresponding accuracy is $|\tilde{\sigma}|_5 \leq (0.51, 2.7, 7.3, 9.6, 7.7, 3.5)$.

The response of EDHD to the noise $\eta = \cos(10^5 t)$ demonstrates its strong approximability features [8] and the accuracy $|\tilde{\sigma}|_5 \leq (0.014, 0.13, 0.61, 1.43, 1.63, 0.98)$. The corresponding accuracy of the EDD is $|\tilde{\sigma}|_5 \leq (0.043, 0.29, 0.90, 1.17, 0.71, 0.51)$.

6.3 *Triggered measurements and variable L*

Consider the inputs

$$\begin{aligned} &f_0(t) = \cos^4 t + 1.003,\ f(t_k) = f_0(t_k) + \eta(t_k), \\ &L_0(t) = 40 + 240\cos^2 t,\ L(t_k) = L_0(t_k). \end{aligned} \tag{29}$$

It is easy to check that $f_0^{(4)}(t) = 256\cos^4 t - 240\cos^2 t + 24$, $|f_0^{(4)}(t)| \leq 40 < L_0(t)$, $\dot{L}_0 \leq 2L_0$, $M = 2$ (Fig. 7a).

Apply the third-order hybrid differentiator (9), (8). According to Theorem 6 intermediate integration steps do not influence the accuracy assymptotics of the discrete hybrid differentiator HDHD (26). Thus, take $l_k = 1$, $\underline{\tau}_{k,j} = \tau_k$, whereas always $j = 0$. The corresponding one-step discretization (26) produces the ready-to-use recursive discrete filter HDHD

$$\begin{aligned}
&z_0(t_{k+1}) = z_0(t_k) + v_0(t_k)\tau_k + \tfrac{1}{2}z_2(t_k)\tau_k^2 + \tfrac{1}{6}z_3(t_k)\tau_k^3, \\
&v_0(t_k) = -3L(t_k)^{1/4}\lfloor z_0(t_k) - f(t_k)\rceil^{3/4} \\
&\qquad\qquad -5M(z_0(t_k) - f(t_k)) + z_1(t_k), \\
&z_1(t_{k+1}) = z_1(t_k) + v_1(t_k)\tau_k + \tfrac{1}{2}z_3(t_k)\tau_k^2, \\
&v_1(t_k) = -2L(t_k)^{1/3}\lfloor z_1(t_k) - v_0(t_k)\rceil^{2/3} \\
&\qquad\qquad -4M(z_1(t_k) - v_0(t_k)) + z_2(t_k), \\
&z_2(t_{k+1}) = z_2(t_k) + v_2(t_k)\tau_k, \\
&v_2(t_k) = -1.5L(t_k)^{1/2}\lfloor z_2(t_k) - v_1(t_k)\rceil^{1/2} \\
&\qquad\qquad -3M(z_2(t_k) - v_1(t_k)) + z_3(t_k), \\
&z_3(t_{k+1}) = z_3(t_k) - 1.1L(t_k)\,\mathrm{sign}(z_3(t_k) - v_2(t_k))\tau_k \\
&\qquad\qquad -2M(z_3(t_k) - v_2(t_k))\tau_k.
\end{aligned} \tag{30}$$

Let $z(0) = (1000, -1000, 1200, 10000)$. First demonstrate the convergence of differentiator (30) with $\tau_k = \underline{\tau}_{k,j} = 10^{-5}$. It approximately corresponds to differentiator (9), (8) with continuous exact measurements. The convergence is very fast and takes 4 time units (Fig. 6). The accuracies over the time interval $[7, 15]$ are described by the component-wise inequality $|\tilde{\sigma}|_3 = (|z_0 - f_0|, |z_1 - \dot{f}_0|, |z_2 - \ddot{f}_0|, |z_3 - \dddot{f}_0|) \leq (1.3 \cdot 10^{-15}, 9 \cdot 10^{-11}, 2.4 \cdot 10^{-6}, 0.03)$.

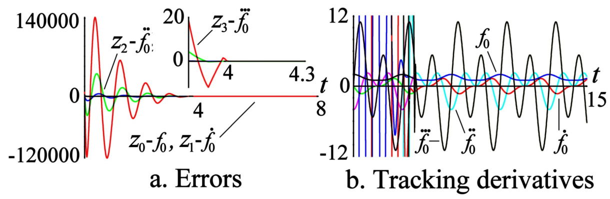

Fig. 6. Convergence of the hybrid differentiator (30) for the initial values $z(0) = (1000, -1000, 1200, 10000)$ with exact uniform sampling. a: differentiation errors, b: comparison of the estimated and exact derivatives, graphs are cut from above and from below.

Triggered measurements. Let $\lfloor A \rfloor$ denote the maximal integer not exceeding A, $\varepsilon_T > 0$ be the sensitivity threshold. Let the sensor produce the measurement $f(t_k) = \lfloor f_0(t)/\varepsilon_T \rfloor \varepsilon_T$ at each time t_k as it detects the change of the integer number $\lfloor f_0(t)/\varepsilon_T \rfloor$ (Fig. 7c).

Let now the integration step be $\tilde{\tau} > 0$, and the sensor check the value of $f_0(t)$ with the same time step $\tilde{\tau}$. Hence, the measurement also contains a small quantization noise $\eta(t_k) = f(t_k) - f_0(t_k)$, $|\eta(t_k)| \leq \max[\varepsilon_T, |\dot{f}_0(t_k)|\tilde{\tau} + \sup|\ddot{f}_0|\tilde{\tau}^2]$.

Let the sensor sensitivity parameter be $\varepsilon_T = 0.01$, $\tilde{\tau} = 0.0001$. The resulting triggered sampling step varies between 0.0001 and 0.43 (Fig. 7b). It is a piece-wise-constant function with peaks at the points with $\dot{f}_0 = 0$.

Direct application of the hybrid differentiator (30) with the same large initial conditions leads to the immediate explosion (Fig. 7d). For initial conditions $||z(0)|| \leq 20$ the differentiator demonstrates the practical stability with $|\tilde{\sigma}|_3 \leq (1.7, 34, 270, 1265)$.

Now introduce virtual measurements artificially keeping the sampling interval not exceeding 0.001. The resulting

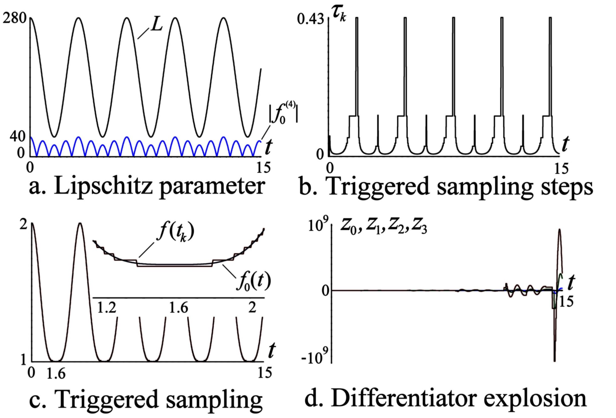

Fig. 7. Triggered sampling causes explosion. a: Graphs of the function $L(t)$ and $|f_0^{(4)}(t)|$; b: the triggered sensor sampling intervals; c: function $f_0(t)$ and sampled values $f(t_k)$, a zoom is also presented; d: explosive divergence of the hybrid differentiator (30) due to the triggered sampling for the initial values $z(0) = (1000, -1000, 1200, 10000)$.

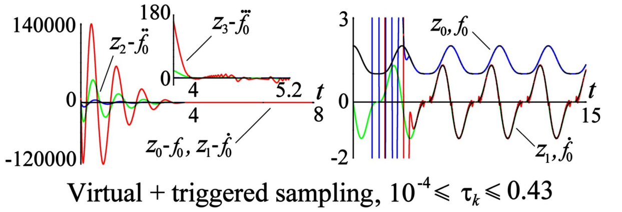

Fig. 8. Convergence of the hybrid differentiator (30) for the initial values $z(0) = (1000, -1000, 1200, 10000)$ with virtual measurements and triggered sampling. Left: differentiation errors, Right: comparison of the estimated and exact derivatives, the graphs are cut from above and from below. Only estimations of $f_0, \dot{f}_0$ are shown on the right.

performance is demonstrated in Fig. 8b. The corresponding accuracy is $|\tilde{\sigma}|_3 \le (0.007, 0.28, 4, 28)$. The accuracy does not significantly change for the virtual measurements keeping the variable upper sampling-interval bound $\tau_T = 0.1(\varepsilon_T/L(t))^{1/4}$.

7 Conclusions and further research directions

Discretization schemes of SM-based homogeneous and non-homogeneous "hybrid" differentiators with variable and constant Lipschitz parameters are considered. For the first time the influence of the numerical integration between the sampling instants is studied.

The new homogeneous discretization (16)-(18) extends results [30] and restores the optimal accuracy asymptotics of the continuous-time differentiaton.

The proposed virtual sampling preserves the same accuracy asymptotics in the case of triggered measurements.

In the case of the constant Lipschitz parameter L one can choose between the homogeneous discretization of the standard differentiator (16) and the hybrid differentiator (25). The latter features global fast FT convergence, but can lose its stability if sampling steps are too large. The first one is extremely stable, but slowly converges from a large error.

The results are directly extendable to the filtering differentiators [25,28] which reject some *unbounded* noises.

Acknowledgment. The authors highly appreciate the comment by the anonymous reviewer on the exact discretization option (20).

8 Appendix: Preliminaries. Accuracy of disturbed homogeneous DIs

Consider a disturbed DI

$$\dot{x} \in F(x, \pi),\ x \in \mathbb{R}^{n_x},\ \pi \in \mathbb{R}^{\nu}, \tag{31}$$

where π is the vector disturbance parameter. The set field $F(x,\pi) \subset T_x\mathbb{R}^{n_x}$ is a non-empty compact convex set-valued function, upper-semicontinuous at all points $(x, 0)$, $x \in \mathbb{R}^{n_x}$.

Introduce the dilations

$$d_\kappa : (x_1, ..., x_{n_x}) \mapsto (\kappa^{m_1} x_1, ..., \kappa^{m_{n_x}} x_{n_x}),\ m_1, ..., m_{n_x} > 0,$$

$$\Delta_\kappa : (\pi_1, ..., \pi_\nu) \mapsto (\kappa^{m_{\pi 1}} \pi_1, ..., \kappa^{m_{\pi\nu}} \pi_\nu),\ m_{\pi 1}, ..., m_{\pi\nu} > 0.$$

Inclusion (31) is assumed homogeneous in both x and π, while the undisturbed DI $\dot{x} \in F(x, 0)$ is assumed FT stable of the homogeneity degree $q = -p$, $p > 0$. Hence, $m_i \ge p$.

The homogeneity of DI (31) means that the transformation $(t, x, \pi) \mapsto (\kappa^p t, d_\kappa x, \Delta_\kappa \pi)$, $\kappa > 0$, establishes a one-to-one correspondence between the solutions of the DI (31) with parameters π and $\Delta_\kappa \pi$. In other words, $F(x, \pi) = \kappa^p d_\kappa^{-1} F(d_\kappa x, \Delta_\kappa \pi)$. In particular, the standard homogeneity $F(x, 0) = \kappa^p d_\kappa^{-1} F(d_\kappa x, 0)$ is obtained for $\pi = 0$.

In its turn $\pi \in \Pi(\omega, x) \subset \mathbb{R}^\nu$, where Π is a homogeneous compact non-empty set-valued function with the magnitude parameter $\omega \ge 0$, i.e. $\forall \kappa, \omega > 0 \forall x \in \mathbb{R}^{n_x}$: $\Pi(\kappa^{m_\omega}\omega, d_\kappa x) = \Delta_\kappa \Pi(\omega, x)$, $m_\omega > 0$. The function Π monotonically increases with respect to the parameter ω, i.e. $0 \le \omega \le \hat{\omega}$ implies $\Pi(\omega, x) \subset \Pi(\hat{\omega}, x)$. It is also assumed that $\Pi(0, x) = \{0\} \subset \mathbb{R}^{n_x}$ and $\Pi(\omega, x)$ is Hausdorff-continuous [4] in ω, x at the points $(0, x)$.

Obviously, the transformation $(t, \omega, x) \mapsto (\kappa^p t, \kappa^{m_\omega}\omega, d_\kappa x)$ establishes a one-to-one correspondence between the solutions of $\dot{x} \in F(x, \Pi(\omega, x))$ with different values of ω.

Now, consider the general retarded DI

$$\dot{x} \in F(x(t - \varpi[0,1]), \Pi(\omega, x(t - \varpi[0,1]))), \tag{32}$$

where $\varpi \ge 0$ is the maximal possible time delay. Moreover, we allow each coordinate x_i of x to have its own different independent delay at each of its two appearances on the right.

The presence of the delays requires some functional initial conditions [23], which can be canceled in our case, since the dynamics are not affected by the state values for $t < 0$. Indeed, the first sampling is at $t = 0$.

The existence of **some** solutions of (32) is obvious. Notably, the solutions with velocity $\dot{x}$ frozen between the "sampling instants", $\dot{x}(t) = \dot{x}(t_k) \in F(x(t_k), \Pi(\omega, x(t_k)))$ for $t \in [t_k, t_{k+1})$, $t_{k+1} - t_k \le \varpi$, are indefinitely extendable in time.

Theorem 8 ([21,23]) *There exist $\gamma_i > 0$, $i = 1, ..., n_x$, such that for any $\omega, \varpi \ge 0$ each extendable solution of DI (32) after a finite-time transient enters the region $|x_i(t)| \le \gamma_i \delta^{m_i}$, $\delta = \max\{\omega^{1/m_\omega}, \varpi^{1/p}\}$, to stay there forever.*

9 Appendix: Proofs of Theorems 2-4

Proof of Theorem 2. It is given that $\underline{\tau}_{k,j} = \underline{\tau} = const$. Introduce the sequence $f_{k,j} = (f_{k,j}^0, ..., f_{k,j}^n)^T$, where $f_{k,j}^0 = f_0(t_{k,j})$, $f_{k,j+1}^i = (f_{k,j+1}^{i-1} - f_{k,j}^{i-1})/\underline{\tau}$ for $i = 1, 2, ..., n$. It is the sequence of divided differences. It is known that

$$f_{k,j}^i = f_0^{(i)}(\xi_{k,j}),\ \xi_{k,j} \in [t_{k,j-i}, t_{k,j}],\ |f_{k,j}^{n+1}| \le L. \tag{33}$$

The sequence $t_{k,j}$ is naturally formally defined for negative j, e.g. $t_{k,-1} = t_{k-1,l_k-1}$, etc. Obviously, $f^i_{k,j+1} = f^i_{k,j} + f^{i+1}_{k,j+1}\underline{\tau}$, $i = 0,1,...,n$.

Subtract $f_{k,j+1}$ from both sides of (13), and denote $s_{k,j} = (s^0_{k,j},...,s^n_{k,j})^T$, $s^i_{k,j} = (z_i(t_{k,j}) - f^i_{k,j})/L$. It yields

$$\begin{aligned} &s_{k,j+1} \in s_{k,j} + \Delta_n(s^0_{k,0} + [-\varepsilon,\varepsilon], s_{k,j}, \vec{\lambda})\underline{\tau} + \underline{\tau}h_0, \\ &h_0 = (0,...,0,[-1,1])^T. \end{aligned} \tag{34}$$

Note that there is a variable discrete delay of $s^0_{k,0}$ with respect to $s^0_{k,j}$ which does not exceed l_k. System (34) describes the node points of solutions $\vec{s}(t) = (s_0(t),...,s_n(t))^T$ with piece-wise-constant derivatives of the system

$$\dot{\vec{s}}(t) \in \Delta_n(s_0(t-\rho[0,1]) + \rho^{n+1}[-1,1], \vec{s}(t-\rho[0,1]), \vec{\lambda}) + h_0$$

which approximate solutions of the FT stable DI (5). Parameters $\underline{\tau}$, τ, ε define the system disturbance parameter $\rho = \max\{\tau, \varepsilon^{\frac{1}{n+1}}\}$. Therefore, solutions converge into a bounded attractor, whose asymptotics is defined by Theorem 8, $\deg\rho = 1$. Taking into account the features (33) of divided differences and $|f_0^{(i+1)}| \le LD_{i+1}$ obtain

$$f^i_{k,j} = f^{(i)}(\xi_{k,j}) \in f_0^{(i)}(t_{k,j}) + iLD_{i+1}\underline{\tau}[-1,1]$$

and the claimed accuracy. □

Notation. In the rest of Appendix 9 denote

$$s^i_{k,j} = \tfrac{1}{L_0(t_{k,j})}\left(z_i(t_{k,j}) - f_0^{(i)}(t_{k,j})\right),\ s_{k,j} = (s^0_{k,j},...,s^n_{k,j})^T.$$

Recall that if L is assumed constant in the theorem conditions then $L = L_0 = const$.

Proof of Theorem 3. Subtract

$$\begin{aligned} f_0^{(i)}(t_{k,j+1}) \in\ & f_0^{(i)}(t_{k,j}) + f_0^{(i+1)}(t_{k,j})\underline{\tau}_{k,j} \\ & + \tfrac{1}{2}\underline{\tau}^2_{k,j}LD_{i+2}[-1,1],\ i = 0,...,n-1, \\ f_0^{(n)}(t_{k,j+1}) \in\ & f_0^{(n)}(t_{k,j}) + L[-1,1]\underline{\tau}_{k,j},\ i = n \end{aligned}$$

from the both sides of the equation for z_i of (13), divide by $L = L_0$ and get

$$\begin{aligned} s_{k,j+1} \in\ & s_{k,j} + \Delta_n(s^0_{k,0} + [-\varepsilon,\varepsilon], s_{k,j}, \vec{\lambda})\underline{\tau}_{k,j} \\ & + \underline{\tau}_{k,j}h_0 + \underline{\tau}^2_{k,j}h_1, \\ h_1 =\ & \tfrac{1}{2}[-1,1](D_2,...,D_{n+1},0)^T. \end{aligned} \tag{35}$$

Here h_1 presents the disturbance.

Rewrite (35) as nodes of a solution of the disturbed retarded DI (5) with piece-wise constant derivative taking switches at $t_{k,j}$:

$$\begin{aligned} \dot{\vec{\sigma}}(t) \in\ & \Delta_n(\sigma_0(t-\tau[0,1]) \\ & + \varepsilon[-1,1], \vec{\sigma}(t-\tau[0,1]), \vec{\lambda}) + h_0 + \underline{\tau}h_1. \end{aligned} \tag{36}$$

Rewrite solutions of (36) as solutions of the larger DI

$$\begin{aligned} \dot{\vec{\sigma}}(t) \in\ & \Delta_n(\sigma_0(t-\rho[0,1]) + \rho^{n+1}[-1,1], \vec{\sigma}(t-\rho[0,1]), \vec{\lambda}) \\ & + h_0 + \tilde{h}(\tilde{\rho}), \\ \tilde{h}(\tilde{\rho}) =\ & \tfrac{1}{2}[-1,1](\tilde{\rho}^n\underline{\tau}_M D_2, \tilde{\rho}^{n-1}\underline{\tau}_M D_3, ..., \tilde{\rho}\underline{\tau}_M D_{n+1}, 0)^T, \end{aligned} \tag{37}$$

where $\tilde{\rho} = \underline{\tau}_M^{-\frac{1}{n}}\rho = \underline{\tau}_M^{-\frac{1}{n}}\max\{\tau, \varepsilon^{\frac{1}{n+1}}, \underline{\tau}^{\frac{1}{n}}\}$, $\underline{\tau} \le \underline{\tau}_M$, $\deg\rho = 1$. The final accuracy (15) follows now from Theorem 8. □

Proof of Theorem 4. Subtract

$$\begin{aligned} & f_0^{(i)}(t_{k,j+1}) \in f_0^{(i)}(t_{k,j}) + f_0^{(i+1)}(t_{k,j})\underline{\tau}_{k,j} \\ & + ... + \tfrac{1}{(n-i)!}\underline{\tau}^{n-i}_{k,j}f_0^{(n)}(t_{k,j}) + \tfrac{1}{(n+1-i)!}\underline{\tau}^{n+1-i}_{k,j}L[-1,1], \\ & \qquad\qquad\qquad i = 0,...,n-1, \\ & f_0^{(n)}(t_{k,j+1}) \in f_0^{(n)}(t_{k,j}) + L[-1,1]\underline{\tau}_{k,j},\ i = n \end{aligned}$$

from the both sides of the equation for z_i of (16), divide by L and get

$$\begin{aligned} & s_{k,j+1} \in s_{k,j} + \Delta_n(s^0_{k,0} + [-\varepsilon,\varepsilon], s_{k,j}, \vec{\lambda})\underline{\tau}_{k,j} + \underline{\tau}_{k,j}h_0 \\ & + H_n(s_{k,j}, \underline{\tau}_{k,j})\underline{\tau}^2_{k,j} + \hat{H}_n(s_{0,k,j}, \underline{\tau}_{k,j})\underline{\tau}^{\chi+1}_{k,j} + h_2(\underline{\tau}_{k,j}), \\ & h_2 = [-1,1](\tfrac{1}{(n+1)!}\underline{\tau}^{n+1}_{k,j}, ..., \tfrac{1}{3!}\underline{\tau}^3_{k,j}, \tfrac{1}{2}\underline{\tau}^2_{k,j}, 0)^T, \end{aligned} \tag{38}$$

where $s^i_{k,j} = [z_i(t_{k,j}) - f_0^{(i)}(t_{k,j})]/L$. Rewrite (38) as nodes of a solution of the disturbed retarded DI (5) with piece-wise constant velocity taking switches at $t_{k,j}$:

$$\begin{aligned} & \dot{\vec{\sigma}}(t) \in \Delta_n(\sigma_0(t-\tau[0,1]) + \varepsilon[-1,1], \vec{\sigma}(t-\tau[0,1]), \vec{\lambda}) \\ & + h_0 + \underline{\tau}^{-1}_{k,j}h_2(\underline{\tau}_{k,j}) + H_n(s_{k,j}, \underline{\tau}_{k,j})\underline{\tau}_{k,j} + \hat{H}_n(s^0_{k,j}, [0,\tau])\underline{\tau}^{\chi}_{k,j}. \end{aligned} \tag{39}$$

In their turn, solutions of (39) satisfy the larger DI

$$\begin{aligned} & \dot{\vec{\sigma}}(t) \in \\ & \Delta_n(\sigma_0(t-[0,\rho]) + \rho^{n+1}[-1,1], \vec{\sigma}(t-[0,\rho]), \vec{\lambda}) \\ & + h_0 + \tilde{h}(\rho) + H_n(\vec{\sigma}(t-[0,\rho]), [0,\rho])[0,\rho] \\ & + \hat{H}_n(\sigma_0(t-[0,\rho]), [0,\rho])[0,\rho^{\chi}], \\ & \tilde{h}(\rho) = [-1,1](\tfrac{1}{(n+1)!}\rho^n, \tfrac{1}{n!}\rho^{n-1}, ..., \tfrac{1}{2}\rho, 0)^T, \end{aligned} \tag{40}$$

where $\rho = \max\{\tau, \varepsilon^{\frac{1}{n+1}}\}$, $\deg\rho = 1$. The final accuracy follows now from Theorem 8. □

10 Appendix: Proofs of Theorems 5-7

For any function $g(t)$ denote $g_{k,j} = g(t_{k,j})$, $g_k = g(t_k) = g(t_{k,0})$. Also denote $I_\omega = [1-\omega, 1+\omega]$ for $\omega \ge 0$.

Proof of Theorem 5.

1. First consider the case of the simplest discrete differentiator (24) with variable L and equal integration steps.

Fix some t_*, $L_* = L_0(t_*)$ and some time interval $\Delta T > 0$. Then $L_0(t) \in I_{2M\Delta T}L_0(t_*)$ for $t \in [t_* - \Delta T, t_* + \Delta T]$ and ΔT small enough. Obviously $I_{2M\Delta T}$ retracts to $\{1\}$ as $\Delta T \to 0$.

For the equal integrations steps $\underline{\tau}_{k,j} = \underline{\tau}$ similarly to the proof of Theorem 2 denote $s^i_{k,j} = (z_i(t_{k,j}) - f^i_{k,j})/L_*$ and get

$$\begin{aligned} & s_{k,j+1} \in s_{k,j} \\ & \quad + I_{2M\Delta T}\Delta_n(s^0_{k,0} + e^{M\Delta T}[-\varepsilon,\varepsilon], s_{k,j}, \vec{\lambda})\underline{\tau} + \underline{\tau} e^{M\Delta T} h_0, \\ & h_0 = (0,...,0,[-1,1])^T. \end{aligned} \quad (41)$$

Solutions of (41) are approximate solutions of

$$\dot{s} \in I_{2M\Delta T}\Delta_n(s_0, s, \vec{\lambda}) + e^{M\Delta T} h_0, \quad (42)$$

which is FT stable for sufficiently small $\Delta T > 0$ [20,23]. Take now such a vicinity of $s = 0$ that is forward invariant with respect to (42) [20] and all solutions starting within it converge to zero in the time $0.5\Delta T$. The resulting accuracy is obtained from Theorem 8 as in the proof of Theorem 2.

The further proof follows [22]: solutions are extended to infinity by the simple multiplication of s by $L_0(t_*)/L_0(t_* + \Delta T)$ at the end of each ΔT-time interval and the setting of the new value of t_* to $t_* + \Delta T$.

2. Consider the case of the discrete differentiator (24) with variable L and variable integration steps. Denoting $s^i_{k,j} = (z_i(t_{k,j}) - f_0^{(i)}(t_{k,j}))/L_0(t_*)$, $\hat{I} = I_{2M\Delta T + \varepsilon_L}$ obtain

$$\begin{aligned} \dot{\vec{\sigma}}(t) \in \hat{I}\Delta_n(&\sigma_0(t - \tau[0,1]) + e^{M\Delta T}\varepsilon[-1,1], \\ &\vec{\sigma}(t - \tau[0,1]), \vec{\lambda}) + e^{M\Delta T}(h_0 + \underline{\tau} h_1), \\ h_1 = \tfrac{1}{2}&[-1,1](D_2,...,D_{n+1},0)^T. \end{aligned} \quad (43)$$

The further proof is similar to the case 1.

3. Consider the case of the discrete differentiator (23) with variable L and *constant or variable integration steps.* The dynamics in the vicinity of $\vec{\sigma} = 0$ is considered similarly to the cases 1, 2 above.

Indeed, it is easily seen from (8), (10) that for arbitrarily small ε_0 and sufficiently small s_0, ε_L

$$\bar{\phi}_i(s_0) \in -\tilde{\lambda}_{n-i} I_{\varepsilon_0} \lfloor s_0 \rceil^{\frac{n-i}{n+1}}, \quad (44)$$

Now taking sufficiently small ΔT and $t \in [t_* - \Delta T, t_* + \Delta T]$ get for some small ε_1

$$\begin{aligned} & z(t_{k,j+1}) \in z(t_{k,j}) + \\ & L_* I_{\varepsilon_1}\Phi_n(\tfrac{z_0(t_k) - f(t_k)}{L_*}, \tfrac{z(t_{k,j})}{L_*}, M, \vec{\lambda}, \vec{\mu})\underline{\tau}_{k,j} \end{aligned}$$

Consider the *constant integration steps' case*. Repeating the proof 1. above, taking into account (44) and denoting $s^i_{k,j} = (z_i(t_{k,j}) - f^i_{k,j})/L_*$ get

$$\begin{aligned} s_{k,j+1} \in s_{k,j} + I_{\varepsilon_2}\Delta_n(s^0_{k,0} + e^{M\Delta T}[-\varepsilon,\varepsilon], s_{k,j}, \vec{\lambda})\underline{\tau} \\ + \underline{\tau} e^{M\Delta T} h_0, \end{aligned}$$

for some small $\varepsilon_2 > \varepsilon_1 + \varepsilon_0$. The further proof is the same as in case 1. above.

In the same way the case of *variable integration steps* is considered. Respectively, in a small vicinity of $\vec{\sigma} = 0$ the error dynamics is described by the FTS DI

$$\begin{aligned} \dot{\vec{\sigma}}(t) \in I_{\varepsilon_2}\Delta_n(&\sigma_0(t - \tau[0,1]) + e^{M\Delta T}\varepsilon[-1,1], \\ &\vec{\sigma}(t - \tau[0,1]), \vec{\lambda}) + e^{M\Delta T}(h_0 + \underline{\tau} h_1), \\ h_1 = \tfrac{1}{2}&[-1,1](D_2,...,D_{n+1},0)^T. \end{aligned}$$

and the further proof is the same as in case 2.

One still needs to prove the existence of a FT invariant attractor in an arbitrarily small vicinity of $\vec{\sigma} = 0$.

Recall how the convergence of differentiator (11) is proven [24]. A number $R_n > 0$ is chosen, which is further supposed to be small and defining the radius of the above small vicinity. Now it is proved that for some fixed $Q_n \geq 1$, time $T > 0$ and any $R \geq R_n$, all trajectories starting in the ball $B_R = \{\vec{\sigma} | \, ||\vec{\sigma}|| \leq R\}$ in time T concentrate in the ball $B_{R/2}$ to stay there forever. On the way trajectories do not leave the ball $B_{Q_n R}$.

Denote $\zeta_i = \sigma_i/R = \tilde{\sigma}_i/(L_0 R)$, where $\tilde{\sigma}_i = z_i - f_0^{(i)}$. Then, since $\dot{L}_0 \in [-M,M]L_0$, get $\dot{\zeta} \in \dot{\tilde{\sigma}}/(L_0 R) - [-M,M]\zeta$. Thus, from (10),(11) get

$$\dot{\zeta} \in \Phi_n(\zeta_0, \zeta, M, \vec{\lambda}, \vec{\mu}) - [-M,M]\zeta. \quad (45)$$

According to [24] all solutions starting in $||\zeta|| \leq 1$ in time T converge to $||\zeta|| \leq 0.5$ without leaving $||\zeta|| \leq Q_n$ on the way.

Now denoting $L_{k,j} = L_0(t_{k,j})$ (omitting index 0) get the trivial relations

$$\begin{aligned} \tfrac{\tilde{\sigma}_{k,j+1}}{L_{k,j+1}} &= \tfrac{\tilde{\sigma}_{k,j}}{L_{k,j}} + \tfrac{\tilde{\sigma}_{k,j+1} - \tilde{\sigma}_{k,j}}{L_{k,j}} - \tfrac{\tilde{\sigma}_{k,j+1}}{L_{k,j+1}} \tfrac{L_{k,j+1} - L_{k,j}}{L_{k,j}}, \\ \tfrac{\tilde{\sigma}_{k,j+1}}{L_{k,j+1}} &\in \left[e^{-M\underline{\tau}_{k,j}}, e^{M\underline{\tau}_{k,j}}\right]^{-1} \left[\tfrac{\tilde{\sigma}_{k,j}}{L_{k,j}} + \tfrac{\tilde{\sigma}_{k,j+1} - \tilde{\sigma}_{k,j}}{L_{k,j}}\right], \end{aligned}$$

which imply that for $\underline{\tau}$ small enough

$$\zeta_{k,j+1} \in \zeta_{k,j} + \tfrac{\tilde{\sigma}_{k,j+1} - \tilde{\sigma}_{k,j}}{L_{k,j} R} + 2M\underline{\tau}[-1,1]\left[\tfrac{\tilde{\sigma}_{k,j+1} - \tilde{\sigma}_{k,j}}{L_{k,j} R}\right].$$

Obviously $L_0(t + \Delta t) \in I_{2M\Delta t} L_0(t)$ for $\Delta t > 0$. Once more denote $\hat{I} = I_{2M\tau + \varepsilon_L}$. Now (23) implies that

$$\begin{aligned} \tfrac{\tilde{\sigma}_{k,j+1} - \tilde{\sigma}_{k,j}}{L_{k,j} R} \in \hat{I}\Phi_n(\zeta_{0,k,0} + \tfrac{1}{R}\varepsilon, \zeta_{k,j}, M, \vec{\lambda}, \vec{\mu})\underline{\tau}_{k,j} \\ + e^{M\tau}(h_0 + \underline{\tau} h_1), \end{aligned} \quad (46)$$

where $\zeta_{0,k,0}$ is the first component of $\zeta_{k,0}$. It means that solutions of the error equations for (23) are approximated solutions of (45). Respectively solutions starting in $||\zeta|| \leq 1$ in time T converge to $||\zeta|| \leq 0.6$ without leaving $||\zeta|| \leq 2Q_n$ on the way. The further proof is trivial. □

Proof of Theorem 6. The proof is divided into the asymptotics analysis for $\vec{\sigma}$ close to zero which is practically the same as the proof of Theorem 4, and the proof of the convergence into this vicinity, which is very similar to that of the case 3 from the above proof of Theorem 5. The only difference is that (46) is replaced with

$$\begin{aligned} \tfrac{\tilde{\sigma}_{k,j+1} - \tilde{\sigma}_{k,j}}{L_{k,j} R} \in \hat{I}\Phi_n(\zeta_{0,k,0} + \tfrac{1}{R}\varepsilon, \zeta_{k,j}, M, \vec{\lambda}, \vec{\mu})\underline{\tau}_{k,j} \\ + e^{M\tau}[\underline{\tau}_{k,j} h_0 + H_n(\zeta_{k,j}, \underline{\tau}_{k,j}) + h_2(\underline{\tau}_{k,j})], \end{aligned}$$

where h_2 has been introduced in (38). □

Proof of Theorem 7 is straightforward due to Theorems 5, 6. □

References

[1] V. Andrieu, L. Praly, and A. Astolfi. Homogeneous approximation, recursive observer design, and output feedback. *SIAM Journal on Control and Optimization*, 47(4):1814–1850, 2008.

[2] M.T. Angulo, J.A. Moreno, and L.M. Fridman. Robust exact uniformly convergent arbitrary order differentiator. *Automatica*, 49(8):2489–2495, 2013.

[3] A.N. Atassi and H.K. Khalil. Separation results for the stabilization of nonlinear systems using different high-gain observer designs. *Systems & Control Letters*, 39(3):183–191, 2000.

[4] A. Bacciotti and L. Rosier. *Liapunov Functions and Stability in Control Theory*. Springer Verlag, London, 2005.

[5] J.-P. Barbot, D. Boutat, and T. Floquet. An observation algorithm for nonlinear systems with unknown inputs. *Automatica*, 45(8):1970–1974, 2009.

[6] J.-P. Barbot, A. Levant, M. Livne, and D. Lunz. Discrete sliding-mode-based differentiators. In *14th International Workshop on Variable Structure Systems (VSS), 2016*, pages 166–171, 2016.

[7] G. Bartolini, A. Pisano, E. Punta, and E. Usai. A survey of applications of second-order sliding mode control to mechanical systems. *International Journal of Control*, 76(9/10):875–892, 2003.

[8] G. Bartolini, E. Punta, and T. Zolezzi. Approximability properties for second-order sliding mode control systems. *IEEE Transactions on Automatic Control*, 52(10):1813–1825, 2007.

[9] E. Bernuau, D. Efimov, W. Perruquetti, and A. Polyakov. On homogeneity and its application in sliding mode control. *Journal of the Franklin Institute*, 351(4):1866–1901, 2014.

[10] I. Castillo, L. Fridman, and J.A. Moreno. Super-twisting algorithm in presence of time and state dependent perturbations. *International Journal of Control*, 91(11):2535–2548, 2018.

[11] F. Dinuzzo and A. Ferrara. Higher order sliding mode controllers with optimal reaching. *IEEE Transactions on Automatic Control*, 54(9):2126–2136, 2009.

[12] C. Edwards, S.K. Spurgeon, and R.J. Patton. Sliding mode observers for fault detection and isolation. *Automatica*, 36(4):541–553, 2000.

[13] Y. Feng, X. Yu, and Z. Man. Non-singular terminal sliding mode control of rigid manipulators. *Automatica*, 38(12):2159–2167, 2002.

[14] A.F. Filippov. *Differential Equations with Discontinuous Right-Hand Sides*. Kluwer Academic Publishers, Dordrecht, 1988.

[15] L. Fridman, Y. Shtessel, C. Edwards, and X.-G. Yan. Higher-order sliding-mode observer for state estimation and input reconstruction in nonlinear systems. *International Journal of Robust and Nonlinear Control*, 18(4-5):399–412, 2008.

[16] S. Koch, M. Reichhartinger, M. Horn, and L. Fridman. Discrete-time implementation of homogeneous differentiators. *IEEE Transactions on Automatic Control*, (available online), 2019.

[17] A. N. Kolmogoroff. On inequalities between upper bounds of consecutive derivatives of an arbitrary function defined on an infinite interval. *American Mathematical Society Translations, Ser. 1*, 2:233–242, 1962.

[18] A. Levant. Robust exact differentiation via sliding mode technique. *Automatica*, 34(3):379–384, 1998.

[19] A. Levant. Higher order sliding modes, differentiation and output-feedback control. *International J. Control*, 76(9/10):924–941, 2003.

[20] A. Levant. Homogeneity approach to high-order sliding mode design. *Automatica*, 41(5):823–830, 2005.

[21] A. Levant, D. Efimov, A. Polyakov, and W. Perruquetti. Stability and robustness of homogeneous differential inclusions. In *Proc. of the 55th IEEE Conference on Decision and Control, Las-Vegas, December 12-14, 2016*, 2016.

[22] A. Levant and M. Livne. Exact differentiation of signals with unbounded higher derivatives. *IEEE Transactions on Automatic Control*, 57(4):1076–1080, 2012.

[23] A. Levant and M. Livne. Weighted homogeneity and robustness of sliding mode control. *Automatica*, 72(10):186–193, 2016.

[24] A. Levant and M. Livne. Globally convergent differentiators with variable gains. *International Journal of Control*, 91(9):1994–2008, 2018.

[25] A. Levant and M. Livne. Robust exact filtering differentiators. *European Journal of Control*, 2019, available online.

[26] A. Levant, M. Livne, and D. Lunz. On discretization of high order sliding modes. In *L. Fridman, J.P. Barbot, F. Plestan (eds). Recent Trends in Sliding Mode Control*, pages 177–202. IET, 2016.

[27] A. Levant, M. Livne, and X. Yu. Sliding-mode-based differentiation and its application. *IFAC-PapersOnLine*, 50(1):1699–1704, 2017.

[28] A. Levant and X. Yu. Sliding-mode-based differentiation and filtering. *IEEE Transactions on Automatic Control*, 63(9):3061–3067, 2018.

[29] S. Li, H. Du, and X. Yu. Discrete-time terminal sliding mode control systems based on Euler's discretization. *IEEE Transactions on Automatic Control*, 59(2):546–552, 2014.

[30] M. Livne and A. Levant. Proper discretization of homogeneous differentiators. *Automatica*, 50:2007–2014, 2014.

[31] M. Mboup, C. Join, and M. Fliess. Numerical differentiation with annihilators in noisy environment. *Numerical algorithms*, 50(4):439–467, 2009.

[32] J.A. Moreno. On strict Lyapunov functions for some non-homogeneous super-twisting algorithms. *Journal of the Franklin Institute*, 351(4):1902–1919, 2014.

[33] J.A. Moreno and M. Osorio. Strict Lyapunov functions for the super-twisting algorithm. *IEEE Transactions on Automatic Control*, 57(4):1035–1040, 2012.

[34] W. Perruquetti, T. Floquet, and E. Moulay. Finite-time observers: application to secure communication. *Automatic Control, IEEE Transactions on*, 53(1):356–360, 2008.

[35] A. Pisano and E. Usai. Sliding mode control: A survey with applications in math. *Mathematics and Computers in Simulation*, 81(5):954–979, 2011.

[36] F. Plestan, A. Glumineau, and S. Laghrouche. A new algorithm for high-order sliding mode control. *International Journal of Robust and Nonlinear Control*, 18(4/5):441–453, 2008.

[37] A. Polyakov, D. Efimov, and W. Perruquetti. Finite-time and fixed-time stabilization: Implicit Lyapunov function approach. *Automatica*, 51(1):332–340, 2015.

[38] M. Reichhartinger, S.K. Spurgeon, M. Forstinger, and M. Wipfler. A robust exact differentiator toolbox for matlab/simulink. In *The 20th IFAC World Congress, Toulouse, France, Jule 9-15, 2017*, 2017.

[39] Y. Shtessel, M. Taleb, and F. Plestan. A novel adaptive-gain supertwisting sliding mode controller: methodology and application. *Automatica*, 48(5):759–769, 2012.

[40] Y.B. Shtessel and I.A. Shkolnikov. Aeronautical and space vehicle control in dynamic sliding manifolds. *International Journal of Control*, 76(9/10):1000–1017, 2003.

[41] S.K. Spurgeon. Sliding mode observers: a survey. *International Journal of Systems Science*, 39(8):751–764, 2008.

[42] V. Torres-González, T. Sanchez, L.M. Fridman, and J.A. Moreno. Design of continuous twisting algorithm. *Automatica*, 80:119–126, 2017.

[43] S.E. Tuna and A.R. Teel. Homogeneous hybrid systems and a converse Lyapunov theorem. In *45th IEEE Conference on Decision and Control, 2006*, pages 6235–6240, 2006.

[44] V.I. Utkin. *Sliding Modes in Control and Optimization*. Springer Verlag, Berlin, Germany, 1992.

[45] X. Yu and J.X. Xu. Nonlinear derivative estimator. *Electronic Letters*, 32(16):1445–1447, 1996.